Journal of the American College of Cardiology Vol. 50, No. 4, 2007

Published by Elsevier Inc.
ISSN 0735-1097/07/$32.00
doi:10.1016/j.jacc.2007.03.044

Cardiac Imaging

Multislice Computed Tomographic Characteristics of Coronary Lesions in Acute Coronary Syndromes

Sadako Motoyama, MD, PHD,* Takeshi Kondo, MD, PHD,† Masayoshi Sarai, MD, PHD,* Atsushi Sugiura, MD, PHD,* Hiroto Harigaya, MD,* Takahisa Sato, MD, PHD,* Kaori Inoue, MD,* Masanori Okumura, MD,* Junichi Ishii, MD, PHD,* Hirofumi Anno, MD, PHD,‡ Renu Virmani, MD, FACC,§ Yukio Ozaki, MD, PHD,* Hitoshi Hishida, MD, PHD,* Jagat Narula, MD, PHD, FACC¶

Toyoake and Takasaki, Japan; Gaithersburg, Maryland; and Irvine, California

Objectives To evaluate the feasibility of noninvasive assessment of the characteristics of disrupted atherosclerotic plaques, the authors interrogated the culprit lesions in acute coronary syndromes (ACS) by multislice computed tomography (CT).

Background Disrupted atherosclerotic plaques responsible for ACS histopathologically demonstrate large lipid cores and positive vascular remodeling. It is expected that plaques vulnerable to rupture should bear similar imaging signatures by CT.

Methods Either 0.5-mm × 16-slice or 64-slice CT was performed in 38 patients with ACS and compared with 33 patients with stable angina pectoris (SAP) before percutaneous coronary intervention. The coronary plaques in ACS and SAP were evaluated for the CT plaque characteristics, including vessel remodeling, consistency of noncalcified plaque (NCP <30 HU or 30 HU <NCP <150 HU), and spotty or large calcification.

Results In the CT profile of culprit ACS and SAP lesions, the frequency of 30 HU <NCP <150 HU (100% vs. 100%, p = NS) was not different, and large calcification (22% vs. 55%, $p = 0.004$) was significantly more frequent in the stable lesions. Positive remodeling (87% vs. 12%, $p < 0.0001$), NCP <30 HU (79% vs. 9%, $p < 0.0001$), and spotty calcification (63% vs. 21%, $p = 0.0005$) were significantly more frequent in the ACS lesions. Presence of all 3 (i.e., positive remodeling, NCP <30 HU, and spotty calcification) showed a high positive predictive value, and absence of all 3 showed a high negative predictive value for the culprit plaques associated with ACS.

Conclusions The CT characteristics of plaques associated with ACS include positive vascular remodeling, low plaque density, and spotty calcification. It is logical to presume that plaques vulnerable to rupture harbor similar characteristics. (J Am Coll Cardiol 2007;50:319–26) © 2007 by the American College of Cardiology Foundation

Disruption of an atherosclerotic plaque is responsible for at least two-thirds of acute coronary events (1,2). Ruptured plaques are histopathologically characterized by large plaque volumes and large necrotic cores that are covered by attenuated fibrous cap often inflamed with monocyte-macrophage infiltration (3). The vessels are positively remodeled at the site of plaque disruption (4,5). In addition, small calcific concretions in fibrous caps have been shown to contribute to plaque instability (6,7). Plaques vulnerable to rupture are termed thin cap fibroatheroma (TCFA) and show histopathological characteristics similar to disrupted plaques except that the fibrous caps are still intact. Various diagnostic techniques have identified the imaging characteristics of disrupted plaques and proposed that these characteristics may allow recognition of coronary lesions likely to result in acute coronary syndromes (ACS) (3,8,9). Multiple catheter-based techniques, such as intravascular ultrasound (IVUS) (5,10–12), optical coherence tomography (13,14), intravascular magnetic resonance (15,16), and thermography (17,18), have been used for the identification of unstable plaques.

Recent improvements in computed tomography (CT) technology and the advent of the multislice computed tomog-

From the *Department of Cardiology, Fujita Health University, Toyoake, Japan; †Department of Cardiology, Takase Clinic, Takasaki, Japan; ‡Department of Radiology, Fujita Health University, Toyoake, Japan; §International Registry of Pathology, Gaithersburg, Maryland; and the ¶Division of Cardiology, University of California Irvine, Irvine, California. Dr. James E. Muller acted as the Guest Editor for this article.

Manuscript received July 25, 2006; revised manuscript received March 13, 2007, accepted March 15, 2007.

Abbreviations and Acronyms

ACS = acute coronary syndrome
CAG = coronary angiography
CT = computed tomography
ECG = electrocardiogram
IVUS = intravascular ultrasound
MSCT = multislice computed tomography
NCP = noncalcified plaques
NPV = negative predictive values
NSTEMI = non–ST-segment elevation myocardial infarction
PCI = percutaneous coronary intervention
PPV = positive predictive value
SAP = stable angina pectoris
STEMI = ST-segment elevation myocardial infarction
TCFA = thin cap fibroatheroma
UAP = unstable angina pectoris

raphy (MSCT) have spurred interest in noninvasive detection of morphologic characteristics of vulnerable plaques (19–23). To evaluate the feasibility of CT assessment of plaque characteristics, we interrogated the culprit lesions in ACS by MSCT and compared them with atherosclerotic plaques in patients presenting with stable angina pectoris (SAP). Based on the available CT literature and histopathological data, remodeling of the vessel, plaque consistency, and the extent of calcification were evaluated by 0.5-mm × 16-slice or 0.5-mm × 64-slice CT.

Methods

We started the study in 2004 with 0.5-mm × 16-slice CT. After 56 consecutive studies (male, 40; female, 16; age 65 ± 12 years), the same study protocol was initiated with 0.5-mm × 64-slice CT and 15 more patients were added (male, 14; female, 1; age 61 ± 10 years). The study was approved by the institutional review board and the ethics committee, and all patients voluntarily consented to participate in the study protocol.

Patients. Preinterventional CT images were obtained in patients presenting with ACS (ST-segment elevation myocardial infarction [STEMI], non–ST-segment elevation myocardial infarction [NSTEMI], and unstable angina pectoris [UAP]) or SAP. Overall, 441 patients were screened for recruitment of 71 patients (16%) (Fig. 1).

The SAP patients were classified based on the Canadian Cardiovascular Society Classification System. Patients with class 1 or 2 were included as candidates in the SAP group (24). Coronary angiography (CAG) was performed, and the patients with single-vessel disease who were advised to have elective percutaneous coronary intervention (PCI) were enrolled in this study. Culprit lesion was determined based on significant stenosis in CAG. These patients underwent CT examination before PCI. After screening of 149 patients, 33 patients were included.

In the ACS group, patients diagnosed with STEMI, NSTEMI, and UAP were included as follows. A 12-lead electrocardiogram (ECG) and cardiac-specific troponin were performed in all patients presenting to the emergency

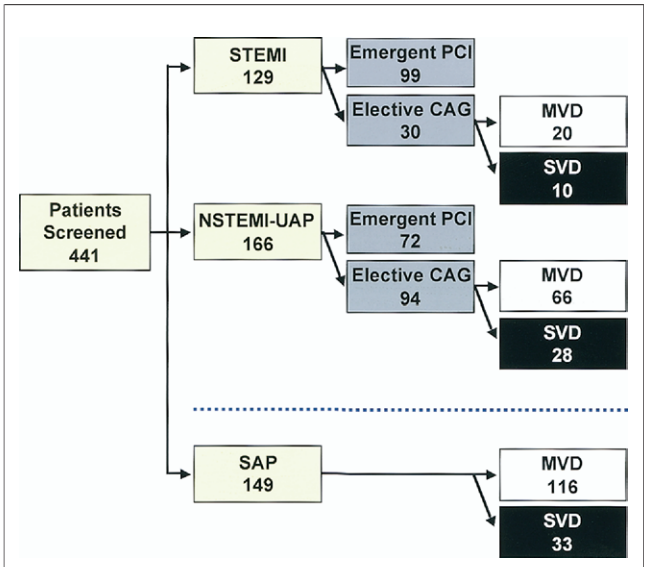

Figure 1 The Patient Population

Overall, 441 patients were screened and 71 were enrolled in the study. Of these 71 patients, 10 had STEMI, 9 had NSTEMI, 19 had UAP, and 33 had SAP. CAG = coronary artery grafting; MVD = multivessel disease; NSTEMI = non–ST-segment elevation myocardial infarction; PCI = percutaneous coronary intervention; SAP = stable angina pectoris; STEMI = ST-segment elevation myocardial infarction; SVD = single-vessel disease; UAP = unstable angina pectoris.

room with chest discomfort. Patients with ischemic discomfort, ST-segment elevation on the ECG, and elevation of troponin level were defined as STEMI. In symptomatic patients with 12-lead ECG ST-segment elevation, reperfusion intervention was initiated as soon as possible without being contingent on a biomarker assay (25); such patients were excluded from the present study. On the other hand, STEMI patients brought to the hospital >24 h after the onset of chest pain and free of symptoms were enrolled in the study.

Patients with ischemic discomfort presenting without ST-segment elevation on the ECG but elevation of troponin level were defined as having NSTEMI. Patients with ischemic discomfort that was Canadian Cardiovascular Society class 3 or 4 without electrocardiographic ST-segment elevation and elevation of troponin level were defined as having UAP. Patients with NSTEMI and UAP were classified into high-, intermediate-, and low-risk groups based on the 2002 American College of Cardiology/American Heart Association UAP/NSTEMI guidelines (26). High-risk patients admitted within 24 h after onset were excluded because these patients needed early CAG and PCI. High-risk patients presenting 24 h after onset of chest pain or intermediate- and low-risk patients were included in the present study. A CAG was performed in all enrolled ACS patients. The culprit lesion was identified on the basis of CAG, location of asynergy in ECG, and location of ST-segment elevation in STEMI. The patients with only

single-vessel disease were enrolled in this study and underwent CT examination before PCI.

Overall 441 patients were screened (Fig. 1), and 71 were enrolled in the study. Of these 71 patients, 10 had STEMI, 9 had NSTEMI, 19 had UAP, and 33 had SAP. The CT plaque characteristics from the culprit ACS and stable lesions were tabulated. Because we have recently reported a comparison of IVUS with plaque composition observed by 16-slice CT (27), we did not feel comfortable performing additional IVUS imaging during coronary catheterization in the first batch of 56 patients. However, we have not reported a comparison of IVUS data with 64-slice CT plaque characteristics earlier. Therefore, we obtained permission for additional IVUS studies in the group of 15 patients studied by 64-slice CT.

MSCT protocol. In the first 56 patients, 16-slice CT (Aquilion 16, Toshiba Medical Systems, Otawara, Japan) was used with collimation 16 × 0.5 mm, detector pitch 3.2 to 3.6, pixel size 0.39 × 0.39 mm, rotation time 400 ms, tube current 360 mA, and voltage 135 kV. For the contrast-enhanced scan, 60 ml of contrast media was injected at 3.0 ml/s followed by 40 ml at 1.5 ml/s. In the remaining 15 patients, 64-slice CT (Aquilion 64) was used with collimation 64 × 0.5 mm; detector pitch 9.8 to 11.2; pixel size 0.39 × 0.39 mm; rotation time 350, 375, or 400 ms; tube current 400 or 450 mA; and voltage 135 kV. For the contrast-enhanced scan, 60 ml contrast media was injected at 4.0 ml/s followed by 20 ml at 2.0 ml/s. This strategy allowed the application of dedicated spiral algorithms that provided up to 75 ms of temporal resolution. The start of contrast-enhanced scan was adapted to sure-start images (28). All scans were performed during a single breath hold. The raw data of the scans were reconstructed using algorithms optimized for retrograde ECG-gated multislice spiral reconstruction. The reconstructed image data of the CT were transferred to a computer workstation for postprocessing (ZIO M900, Amin/ZIO, Tokyo, Japan). For plaque detection, both cross-sectional and curved multiplanar reformation images were analyzed.

Because the rate of infusion of contrast medium was different in the 2 protocols and may affect the diffusion of contrast material into the plaque, we measured the lumen density in both the ACS and the SAP group by 16- and 64-slice CT. Although the Kruskal-Wallis test comparison of the luminal contrast in 4 groups followed by the Fisher protected least significant difference test showed significant difference in the luminal densities in 16- and 64-slice scans, there was no significant difference in the ACS and SAP groups by either 16-slice (262 ± 55 HU vs. 259 ± 29 HU, $p = 0.74$) or 64-slice (318 ± 43 HU vs. 304 ± 51 HU, $p = 0.45$) CT. Therefore, the diffusion of contrast material into the plaques may be different in 16- and 64-slice CT (see plaque consistency), but the comparison of the plaque characteristics between ACS and SAP is valid.

Definition of CT Plaque Characteristics

Vascular remodeling. The coronary arterial remodeling was defined as a change in the vessel diameter at the plaque site in comparison with the reference segment set proximal to the lesion in a normal-appearing vessel segment (reference segment). Manual inspection, in both cross-section and longitudinal reconstruction, was used for defining the remodeling index (lesion diameter/reference diameter). The remodeling index on MSCT was calculated and reported as positive remodeling when the diameter at the plaque site was at least 10% larger than the reference segment. The delineation of the outer vessel boundary was difficult in 6 cases (8%) because of severe calcification.

Plaque consistency. The plaques were reported as either calcified or noncalcified plaques (NCP). Further, based on our comparative 16-slice CT and IVUS data (27), we divided the NCP into 2 categories; NCP <30 HU (corresponding to IVUS lipid cores) and 30 HU <NCP <150 HU (corresponding to IVUS fibrous plaques). Calcification was recognized as the plaque with the density of >220 HU, and was classified as spotty or large calcification. Spotty calcification was defined when <3 mm in size (11) on curved multiplanar reformation images and 1-sided on cross-sectional images. Large calcification was defined as the calcification larger than spotty calcification.

Based on our comparative 16-slice CT and IVUS data (27), the HU density of IVUS-identified soft plaques was 11 ± 12 and that of fibrous plaque was 78 ± 21; there was no overlap in standard deviation values. Accordingly, we established 30 HU as the cutoff point, and IVUS was not performed in patients with 16-slice CT examination. On the other hand, all 15 patients included in the present study with 64-slice CT underwent IVUS examination during coronary angiography; 10 of 15 patients had NCP <30 HU by 64-slice CT. Compared with IVUS, sensitivity and specificity of CT for detecting soft plaque was 91% and 100%. Therefore, we have maintained the value of NCP <30 HU as the cutoff point, and stratified the presence of NCP into 2 groups of NCP <30 HU and 30 HU <NCP <150 HU.

Interpretation of CT scans, data presentation, and statistical analysis. The observers interpreting the CT studies were blinded to the clinical data. Two observers were involved in the interpretation of data, and the interobserver agreement has been calculated by kappa statistic. The agreement (κ) for the interpretation of vascular remodeling and plaque consistency was 0.884 and 0.913 for the 2 observers, respectively. The plaque characteristics were tabulated in ACS and SAP patients, and reported in percent. The sensitivity, specificity, positive and negative predictive values (PPV and NPV), and diagnostic accuracy of each characteristic alone or in combination were calculated. The comparison of the plaque characteristics in the ACS and SAP groups was made using the chi-square test for inde-

Table 1 Clinical and Angiographic Characteristics of the Patients

	ACS (n = 38) (STEMI 10, NSTEMI 9, UAP 19)	SAP (n = 33)	p Value
Age, yrs	62 ± 11	67 ± 9	0.053
Male/female	31/7	23/10	0.242
Diabetes	8 (21%)	7 (22%)	0.987
Hypertension	16 (42%)	19 (58%)	0.295
Hyperlipidemia	23 (61%)	22 (67%)	0.592
Smoking	19 (51%)	18 (55%)	0.702
Obesity	11 (29%)	11 (33%)	0.690
Lesion location			0.650
LAD	19 (50%)	14 (42%)	
LCX	8 (22%)	6 (18%)	
RCA	11 (29%)	12 (36%)	

There was no statistically significant difference in age, gender, presence of risk factors, and coronary vessel involvement between ACS and SAP patient groups.

ACS = acute coronary syndrome; LAD = left anterior descending artery; LCX = left circumflex artery; NSTEMI = non–ST-segment elevation myocardial infarction; RCA = right coronary artery; SAP = stable angina pectoris; STEMI = ST-segment elevation myocardial infarction; UAP = unstable angina pectoris.

pendence, and a p value of <0.05 was considered significant.

Results

The clinical characteristics of all 71 patients are shown in Table 1. There was no statistically significant difference in age, gender, presence of risk factors, or culprit vessel among patients with ACS or SAP.

The characteristics of culprit lesions in ACS and target lesions in SAP are presented in Figures 2 through 4. The CT examination of angiographically defined culprit lesions in ACS revealed positive expansive remodeling of the vessel (87%), NCP <30 HU (79%), and spotty calcification (63%) (Fig. 5). In addition, 30 HU <NCP <150 HU were present in all culprit lesions, and larger calcifications were seen in 22%. On the other hand, the vessels were positively remodeled only in 12% of stable lesions, and all plaques were characterized as 30 HU <NCP <150 HU. Spotty calcification was observed in 21%, but larger calcific plaques were found in 55%. The mean remodeling index in the ACS lesions was 1.20 ± 0.17, which was significantly greater than the SAP plaques (0.96 ± 0.12, $p < 0.0001$).

Although the frequency of 30 HU <NCP <150 HU (100% vs. 100%, p = NS) on the MSCT was not significantly different between the lesions associated with ACS and SAP, large calcification (22% vs. 55%, p = 0.0044) was significantly more frequent in the lesions associated with SAP than ACS. On the other hand, positive remodeling (87% vs. 12%, $p < 0.0001$), NCP <30 HU (79% vs. 9%, $p < 0.0001$), and spotty calcification (63% vs. 21%, p = 0.0005) were significantly more frequent in the culprit ACS lesions than SAP (Fig. 5). The sensitivity, specificity, PPV, and NPV of various characteristics independently or in combination are provided in Table 2. Positive remodeling showed the best sensitivity, specificity, PPV, and NPV of 87%, 88%, 89%, and 85%, respectively. These values for the NCP <30 HU were 79%, 91%, 91%, and 79%, and for spotty calcification were 63%, 79%, 77%, and 65%, respectively. However, when the plaque was described by the absence of all (i.e., positive remodeling, NCP <30 HU, or spotty calcification), NPV was 100%; therefore, plaque associated with an acute event was not missed. On the other hand, when the plaque showed all 3 features (i.e., positive remodel-

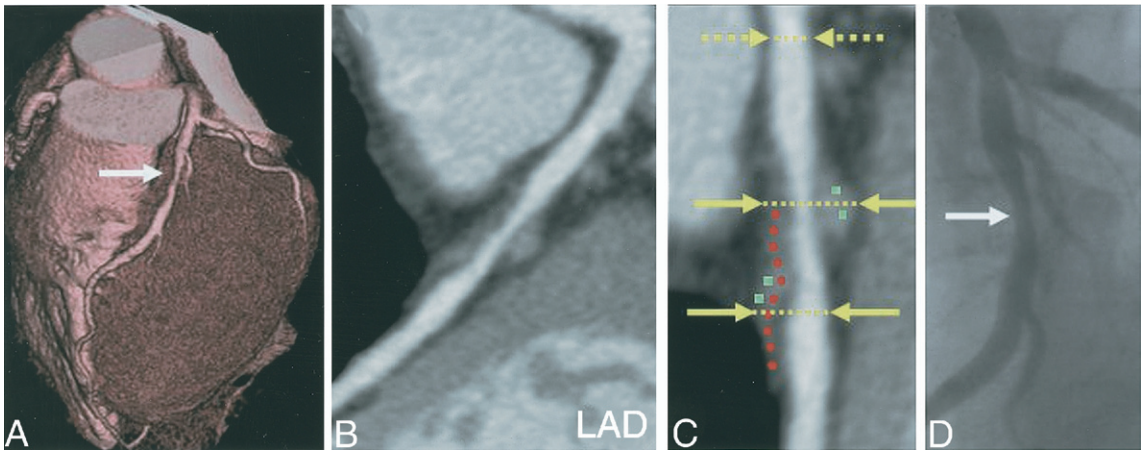

Figure 2 Case 1 With Acute Coronary Syndrome

The CT characteristics of a culprit lesion in a 40-year-old male patient presenting with acute coronary syndrome. **(A)** Volume rendering. **(B)** Curved MPR. **(C)** Magnified view of the region of interest from **(C)**. **(D)** Coronary angiogram. The **white arrows** in **(A)** and **(D)** show the site of luminal obstruction or culprit lesion. As shown by the **solid yellow arrows** at 2 sites in the culprit lesion in **(C)**, the lesion is positively remodeled as compared with the normal coronary segment proximal to the lesion (denoted by **interrupted arrows**). Remodeling index in this patient was 1.43. An NCP <30 HU represents the probability of a soft plaque (**red circles** are placed along the course of low attenuation), and 30 HU <NCP <150 HU denotes a fibrous plaque **(green squares)**. CT = computed tomography; LAD = left anterior descending artery; MPR = multiplanar reformation; NCP = noncalcified plaque.

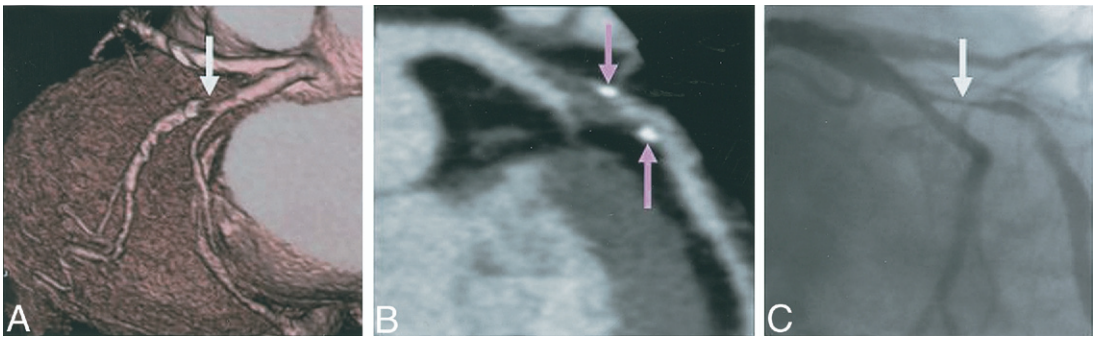

Figure 3 Case 2 With Acute Coronary Syndrome

The CT characteristics of another culprit lesion in a 79-year-old female patient presenting with acute coronary syndrome. **(A)** Volume rendering. **(B)** Curved MPR. **(C)** Coronary angiogram. The **white arrows** in **(A)** and **(C)** show the site of luminal obstruction or culprit lesion. In addition to positive remodeling and NCP plaque (also including areas of <30 HU), spotty calcification **(pink arrows)** is evident. Abbreviations as in Figure 2.

ing, NCP <30 HU, and spotty calcification), the PPV of the plaque associated with an acute event increased to 95%.

Discussion

The present study. The culprit atherosclerotic lesions associated with ACS showed positive vascular remodeling, NCP <30 HU, and spotty calcification on MSCT. These characteristics were uncommonly associated with lesions in patients presenting with SAP. Positive remodeling of the vessel was the most important accompaniment of the culprit lesions and confirms the data described earlier by the IVUS examination (4,5) and the classic pathological description of ruptured plaques on autopsy (2,29,30). The presence of NCP <30 HU offered higher specificity and PPV of 90%, but sensitivity and NPV were <80%. Based on our recent correlation of CT plaque characteristics and IVUS, it is likely that NCP <30 HU represent a necrotic core and may be termed as soft plaque (27). However, extreme caution should be exercised in labeling low-attenuation enclosures in a plaque as a soft plaque or necrotic core. Presence of soft plaque has been described earlier in 1-mm slice thickness MSCT examination as a lesion with <50 HU (22,31). Our data suggest that a lower threshold for soft plaques, especially for MSCT with a 0.5-mm-slice thickness, may improve the specificity of correlation with culprit lesions (27). The diagnostic accuracy for spotty calcification was approximately 70%. Spotty calcification is more likely to be associated with vulnerable plaques, as described earlier by IVUS (11). Presence of all 3 features, including positive remodeling, NCP <30 HU, and spotty calcification, allowed PPV of 95%, providing a high level of confidence for the characterization of a plaque associated with ACS. On the other hand, absence of all 3 features offered an NPV of 100% for the exclusion of culprit lesions by noninvasive

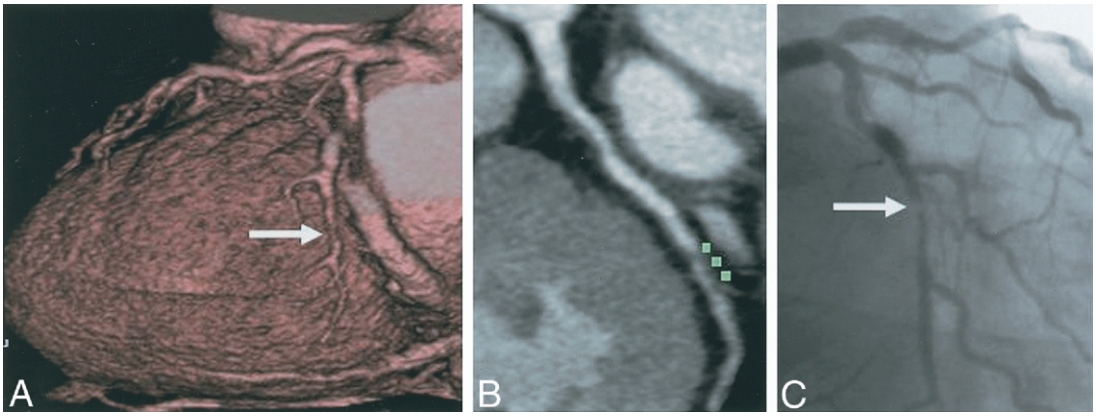

Figure 4 Case 3 With Stable Angina Pectoris

The CT characteristics of a stable plaque from a 77-year-old male patient. The image shows negatively remodeled severely obstructive lesion almost entirely made up of 30 HU <NCP <150 HU **(green squares)**. No NCP <30 HU or spotty calcification is observed. Remodeling index in this patient was 0.87. Abbreviations as in Figure 2.

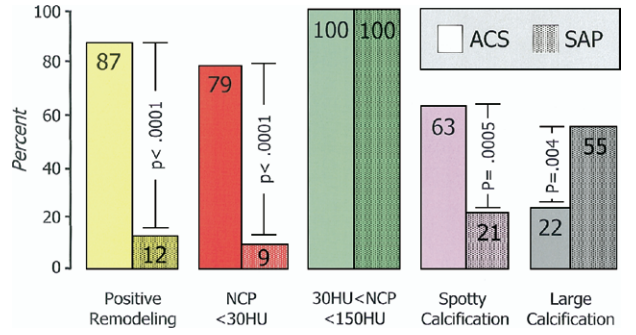

Figure 5 Plaque Characteristics in ACS and SAP

Plaque characteristics of culprit lesions in ACS and target lesions in SAP groups. Positive remodeling, NCP <30 HU, and spotty calcification were more frequently observed in the culprit ACS lesions. ACS = acute coronary syndrome; other abbreviations as in Figure 1.

MSCT imaging. It is reasonable to believe that the CT features of not-yet-disrupted vulnerable plaques should be similar to those of the lesions associated with ACS. It is reasonable to presume that these CT characteristics of a plaque in the absence of an acute coronary event may represent a plaque likely to result in an acute event.

Histomorphologic characteristics of vulnerable plaques. Plaque rupture is the substrate for ACS in at least two-thirds of patients presenting with ACS (1,2,30). Histopathological characteristics of ruptured plaques are well defined, and it has been proposed that the vulnerable plaques harbor the same characteristics (32). It is prudent to discuss these characteristics for defining the expectations from noninvasive imaging modalities (33). The plaque and necrotic core size are described as the most important determinants of the plaque vulnerability. The larger the plaque extent and necrotic core size, the higher is the likelihood of vulnerability of the plaque to rupture. The pathological characterization of ruptured plaques (disrupted and healed ruptures) shows that three-fourths of ruptured plaques occupy >50% cross-sectional vessel area and one-half involve >75% (34). The necrotic core in a given plaque often occupies >25% of the plaque area in at least two-thirds of disrupted lesions (2,34). Although plaque volume is often enormous, plaque burden usually does not compromise lumen size unless 40% or greater cross-sectional vascular area narrowing has occurred (6). Sparing of the lumen occurs because of a positive or outward remodeling of the vessel (2,35). Therefore, angiographic encroachment of the lumen often has been shown to be minimal, and angiographic luminal assessment does not correlate well with the incidence of ACS (36). In particular, lesions with hemorrhage, large necrotic cores, macrophage inflammation, and calcification are more likely to show positive vascular remodeling. On the other hand, stable plaques or plaques associated with nonrupture-related ACS (such as plaque erosion) show no expansive remodeling or rather arterial shrinkage. The expansive growth of vessel offers an easy target for structural imaging. Further, pathological data have clarified that the number of vulnerable plaques present in any given patient is small (34,37). Finally, the majority of TCFAs occur predominantly in the proximal or mid-portion of the 3 major coronary arteries. Because the vulnerable plaques are often sizable, not abundant and located proximally in major vessels, an effort to detect vulnerable plaques is justifiable.

Clinical implications of CT-based detection of plaque vulnerability. Currently, the risk of coronary syndrome is assessed by Framingham score (33). A risk of developing an ACS of <0.5% per year is considered to be low risk, risk of 0.5% to 2.0% per year is intermediate, and >2% per year is often considered to be high risk. Whereas the low-risk group deserves behavioral counseling and follow-up, additional testing is advised for further risk stratification of subjects at intermediate risk (33). The additional tests, such as C-reactive protein, ankle-brachial index, or carotid artery intimal-medial wall thickness, may up-stage the subject to the high-risk category. The latter subjects would include those with multiple risk factors or evident coronary, cerebral, or peripheral vascular disease or who suffer from diabetes mellitus or renal dysfunction (33). Although such patients (vulnerable patients) deserve intense global risk factor reduction, they may constitute the most appropriate population to be subjected to MSCT for potential identification of vulnerable plaques. Identification of such plaques

Table 2 CT Characteristics of Culprit Lesions in ACS and Target Lesions in SAP

	Sensitivity (%)	Specificity (%)	Positive Predictive Value (%)	Negative Predictive Value (%)	Accuracy (%)
Positive remodeling	87	88	89	85	88
NCP <30 HU	79	91	91	79	85
Spotty calcification	63	79	77	65	72
Positive remodeling + NCP <30 HU	74	93	93	76	83
Positive remodeling + NCP <30 HU + spotty calcification	47	97	95	60	70
Positive remodeling or NCP <30 HU	92	85	89	90	89
Positive remodeling or NCP <30 HU or spotty calcification	100	67	78	100	85

CT = computed tomography; NCP = noncalcified plaque; other abbreviations as in Table 1.

may place these subjects at a very high risk (probably in excess of 15%) of developing acute coronary events per year. This will be the key goal for coronary imaging (33).

Study limitations. The analysis entirely based on the density (HU) of various plaque components, such as soft plaque, would have flaws. It is very difficult to differentiate the thrombus from soft plaques and fibrous plaques. We cannot exclude the possibility that in some lesions, thrombosis may have been present, being indistinguishable from the culprit plaque. It is also very difficult to differentiate between lipid-rich and fibrous plaques only on the basis of plaque attenuation, especially as the lesions are often intermixed. The new analytic programs, such as those based on clustering methods, could possibly improve the ability to identify soft plaques in the future; expected improvement in slice thickness should also improve resolution. Lumen density was different between 16- and 64-slice CT, which could reduce sensitivity for the detection of soft plaques. The IVUS study in the latter patients, however, shows >90% sensitivity.

Another limitation of the study arises from the assumption that vulnerable plaques would show characteristics similar to those of already-disrupted plaques. Pathological and IVUS definitions of vulnerable plaques all have been based on the disrupted plaques. Long-term and prospective natural history study of the vascular lesions characterized by CT examination will be required for the precise definition of unstable lesions.

Finally, the number of patients included is small and does not allow development of quantitative parameters, such as the extent of remodeling, plaque size/volume, and proportional occupation of the plaque volume by the necrotic core. It is expected that the advent of 64-slice CT will increase the number of scans performed in patients presenting with ACS in the emergency room. As a larger number of cases become available, it would be possible to offer a more quantitative approach to the detection of unstable coronary lesions.

Conclusions

The CT characteristics of culprit lesions associated with ACS seem to be distinct from those of stable plaques. These characteristics include positive vascular remodeling, presence of low-attenuation NCP, and spotty calcification. It is logical to propose that plaques vulnerable to rupture should harbor similar characteristics and be amenable to noninvasive CT imaging.

Reprint requests and correspondence: Dr. Sadako Motoyama, 1-98 Dengakugakubo, Kutsukake-cho, Toyoake, Aichi, 470-1192, Japan. E-mail: sadakom@fujita-hu.ac.jp.

REFERENCES

1. Davies MJ. The composition of coronary-artery plaques. N Engl J Med 1997;336:1312–4.
2. Burke AP, Farb A, Malcom GT, Liang YH, Smialek J, Virmani R. Coronary risk factors and plaque morphology in men with coronary disease who died suddenly. N Engl J Med 1997;336:1276–82.
3. Narula J, Finn AV, Demaria AN. Picking plaques that pop. J Am Coll Cardiol 2005;45:1970–3.
4. Schoenhagen P, Ziada KM, Kapadia SR, Crowe TD, Nissen SE, Tuzcu EM. Extent and direction of arterial remodeling in stable versus unstable coronary syndromes: an intravascular ultrasound study. Circulation 2000;101:598–603.
5. Hassani S-E, Mintz GS, Fong HS, et al. Negative remodeling and calcified plaque in octogenarians with acute myocardial infarction: an intravascular ultrasound analysis. J Am Coll Cardiol 2006;47:2413–9.
6. Naghavi M, Libby P, Falk E, et al. From vulnerable plaque to vulnerable patient: a call for new definitions and risk assessment strategies: part II. Circulation 2003;108:1772–8.
7. Schaar JA, Muller JE, Falk E, et al. Terminology for high-risk and vulnerable coronary artery plaques. Report of a meeting on the vulnerable plaque, June 17 and 18, 2003, Santorini, Greece. Eur Heart J 2004;25:1077–82.
8. Narula J, Willerson JT. Prologue: detection of vulnerable plaque. J Am Coll Cardiol 2006;47:C1.
9. Muller JE, Tawakol A, Kathiresan S, Narula J. New opportunities for identification and reduction of coronary risk: treatment of vulnerable patients, arteries, and plaques. J Am Coll Cardiol 2006;47:C2–6.
10. Maehara A, Mintz GS, Bui AB, et al. Morphologic and angiographic features of coronary plaque rupture detected by intravascular ultrasound. J Am Coll Cardiol 2002;40:904–10.
11. Ehara S, Kobayashi Y, Yoshiyama M, et al. Spotty calcification typifies the culprit plaque in patients with acute myocardial infarction: an intravascular ultrasound study. Circulation 2004;110:3424–9.
12. Sano K, Kawasaki M, Ishihara Y, et al. Assessment of vulnerable plaques causing acute coronary syndrome using integrated backscatter intravascular ultrasound. J Am Coll Cardiol 2006;47:734–41.
13. Jang IK, Tearney GJ, MacNeill B, et al. In vivo characterization of coronary atherosclerotic plaque by use of optical coherence tomography. Circulation 2005;111:1551–5.
14. Stamper D, Weissman NJ, Brezinski M. Plaque characterization with optical coherence tomography. J Am Coll Cardiol 2006;47:C69–79.
15. Schneiderman J, Wilensky RL, Weiss A, et al. Diagnosis of thin-cap fibroatheromas by a self-contained intravascular magnetic resonance imaging probe in ex vivo human aortas and in situ coronary arteries. J Am Coll Cardiol 2005;45:1961–9.
16. Wilensky RL, Song HK, Ferrari VA. Role of magnetic resonance and intravascular magnetic resonance in the detection of vulnerable plaques. J Am Coll Cardiol 2006;47:C48–56.
17. Toutouzas K, Drakopoulou M, Mitropoulos J, et al. Elevated plaque temperature in non-culprit de novo atheromatous lesions of patients with acute coronary syndromes. J Am Coll Cardiol 2006;47:301–6.
18. Madjid M, Willerson JT, Casscells SW. Intracoronary thermography for detection of high-risk vulnerable plaques. J Am Coll Cardiol 2006;47:C80–5.
19. Schuijf JD, Bax JJ, Jukema JW, et al. Feasibility of assessment of coronary stent patency using 16-slice computed tomography. Am J Cardiol 2004;94:427–30.
20. Hoffmann MH, Shi H, Schmitz BL, et al. Noninvasive coronary angiography with multislice computed tomography. JAMA 2005;293:2471–8.
21. Raff GL, Gallagher MJ, O'Neill WW, Goldstein JA. Diagnostic accuracy of noninvasive coronary angiography using 64-slice spiral computed tomography. J Am Coll Cardiol 2005;46:552–7.
22. Cordeiro MAS, Lima JAC. Atherosclerotic plaque characterization by multidetector row computed tomography angiography. J Am Coll Cardiol 2006;47:C40–7.
23. Hoffmann U, Moselewski F, Nieman K, et al. Noninvasive assessment of plaque morphology and composition in culprit and stable lesions in acute coronary syndrome and stable lesions in stable angina by multidetector computed tomography. J Am Coll Cardiol 2006;47:1655–62.
24. Gibbons RJ, Balady GJ, Bricker JT, et al. ACC/AHA 2002 guideline update for exercise testing: summary article. A report of the American College of Cardiology/American Heart Association Task Force on Practice Guidelines (Committee to Update the 1997 Exercise Testing Guidelines). J Am Coll Cardiol 2002;40:1531–40.

25. Antman EM, Anbe DT, Armstrong PW, et al. ACC/AHA guidelines for the management of patients with ST-elevation myocardial infarction—executive summary. A report of the American College of Cardiology/American Heart Association Task Force on Practice Guidelines (Writing Committee to revise the 1999 guidelines for the management of patients with acute myocardial infarction). J Am Coll Cardiol 2004;44:671–719.
26. Braunwald E, Antman EM, Beasley JW, et al. ACC/AHA 2002 guideline update for the management of patients with unstable angina and non-ST-segment elevation myocardial infarction—summary article: a report of the American College of Cardiology/American Heart Association Task Force on Practice Guidelines (Committee on the Management of Patients With Unstable Angina). J Am Coll Cardiol 2002;40:1366–74.
27. Motoyama S, Kondo T, Anno H, et al. Atherosclerotic plaque characterization by 0.5-mm-slice multislice computed tomographic imaging. Circ J 2007;71:363–6.
28. Anno H, Katada K, Kato R, et al. Scan timing control in contrast helical CT studies using the real-time reconstruction technique—development of sure start function. Med Rev 1997;60:5–12.
29. Varnava AM, Mills PG, Davies MJ. Relationship between coronary artery remodeling and plaque vulnerability. Circulation 2002;105:939–43.
30. Virmani R, Burke AP, Farb A, Kolodgie FD. Pathology of the vulnerable plaque. J Am Coll Cardiol 2006;47:C13–8.
31. Schroeder S, Kopp AF, Baumbach A, et al. Noninvasive detection and evaluation of atherosclerotic coronary plaques with multislice computed tomography. J Am Coll Cardiol 2001;37:1430–5.
32. Kolodgie FD, Virmani R, Burke AP, et al. Pathologic assessment of the vulnerable human coronary plaque. Heart 2004;90:1385–91.
33. Braunwald E. Epilogue: what do clinicians expect from imagers? J Am Coll Cardiol 2006;47:C101–3.
34. Virmani R, Kolodgie FD, Burke AP, Farb A, Schwartz SM. Lessons from sudden coronary death: a comprehensive morphological classification scheme for atherosclerotic lesions. Arterioscler Thromb Vasc Biol 2000;20:1262–75.
35. McPherson DD, Sirna SJ, Hiratzka LF, et al. Coronary arterial remodeling studied by high-frequency epicardial echocardiography: an early compensatory mechanism in patients with obstructive coronary atherosclerosis. J Am Coll Cardiol 1991;17:79–86.
36. Ambrose JA. Plaque disruption and the acute coronary syndromes of unstable angina and myocardial infarction: if the substrate is similar, why is the clinical presentation different? J Am Coll Cardiol 1992;19:1653–8.
37. Ridker PM, Rifai N, Rose L, Buring JE, Cook NR. Comparison of C-reactive protein and low-density lipoprotein cholesterol levels in the prediction of first cardiovascular events. N Engl J Med 2002;347:1557–65.